SCIENCE CHINA
Earth Sciences

• RESEARCH PAPER •

March 2010 Vol.53 No.3: 327–334
doi: 10.1007/s11430-010-0041-z

SIMS Pb/Pb dating of Zr-rich minerals in lunar meteorites Miller Range 05035 and LaPaz Icefield 02224: Implications for the petrogenesis of mare basalt

ZHANG AiCheng[1], HSU WeiBiao[2*], LI QiuLi[3], LIU Yu[3], JIANG Yun[1] & TANG GuoQiang[3]

[1] *Lunar and Planetary Science Center, Purple Mountain Observatory, Chinese Academy of Sciences, Nanjing 210008, China;*
[2] *Faculty of Earth Sciences, China University of Geosciences, Wuhan 430074, China;*
[3] *State Key Laboratory of Lithospheric Evolution, Institute of Geology and Geophysics, Chinese Academy of Sciences, Beijing 100029; China*

Received November 6, 2009; accepted February 3, 2010

Miller Range (MIL) 05035 and LaPaz Icefield (LAP) 02224 are unbrecciated lunar basalt meteorites. In this report, we studied their petrography and mineralogy and made *in situ* uranogenic Pb/Pb dating of Zr-rich minerals. Petrography and mineralogy of these two lunar meteorites are consistent with previous investigations. The zirconolite Pb/Pb age of MIL 05035 is 3851±8 Ma (2σ), in excellent agreement with previous reports. This age suggests that MIL 05035 could be paired with Asuka 881757, a low-Ti mare basalt meteorite. The magmatic event related to MIL 05035 was probably due to the late heavy impact bombardment on the moon around 3.9 Ga. One baddeleyite grain in LAP 02224 shows a large variation of Pb/Pb age, from 3109±29 to 3547±21 Ma (2σ), much older than the whole-rock age of the same meteorite (~3.02±0.03 Ga). The other baddeleyite grain in LAP 02224 has an age of 3005±17 Ma (2σ). The result indicates that the minimum crystallization age of LAP 02224 is ~3.55 Ga and the younger ages could reflect late thermal disturbance on U-Pb system.

Pb/Pb dating, SIMS, zirconolite and baddeleyite, lunar meteorite, low-Ti mare basalt

Citation: Zhang A C, Hsu W B, Li Q L, et al. SIMS Pb/Pb dating of Zr-rich minerals in lunar meteorites Miller Range 05035 and LaPaz Icefield 02224: Implications for the petrogenesis of mare basalt. Sci China Earth Sci, 2010, 53: 327−334, doi: 10.1007/s11430-010-0041-z

1 Introduction

Lunar basalt samples are valuable for understanding magmatic events and internal evolution of the moon. Crystallization ages of lunar basalts can constrain thermal history and crust evolution of the moon (e.g., refs. [1, 2]). However, due to possible disturbance of radiogenic isotopes by complex impact events on the lunar surface, determination of pristine crystallization ages of lunar basalts is not an easy task. In addition, unlike lunar samples collected by Apollo and LUNA missions, the exact locations on the lunar surface of lunar meteorites are unknown, and furthermore the possibility of pairing exists among different meteorites (e.g., LaPaz Icefield lunar meteorites from Antarctica [3]). Therefore, a reliable dating method is crucial to understand thermal history recorded in lunar meteorites and possible pairing among different samples. In lunar basalts, Zr-rich minerals, such as zirconolite, baddeleyite, and tranquillityite, usually occur as late-stage magmatic phases [4] and therefore their ages could represent crystallization ages of mare basalts. Compared to those silicate minerals that are used for Sm-Nd and Rb-Sr isochron and Ar/Ar dating, Zr-rich minerals (e.g., zircon, baddeleyite) have more stable crystal structures and their ages could be closer to pristine igneous crystallization ages. To further understand crystallization

*Corresponding author (email: wbxu@pmo.ac.cn)

ages of mare basalts and possible effect of shock metamorphism on Pb/Pb ages of Zr-rich minerals, we measured Pb/Pb ages of zirconolite and baddeleyite in two lunar basalt meteorites, Miller Range (MIL) 05035 and LaPaz Icefield (LAP) 02224 by using the method developed by Li et al. [5] and discuss the implications for their petrogenesis.

2 Samples and analytical methods

MIL 05035 and LAP 02224 are two unbrecciated crystalline lunar meteorites collected from Antarctica in 2005 and 2002 respectively by the Antarctica Search for Meteorite Program (ANSMET). MIL 05035 weighs 142.2 g and is a very low-Ti basalt (0.9 wt% [6]; 1.44 wt% [7]). LAP 02224 weighs 252.2 g and is a low-Ti basalt (2.94 wt%–3.43 wt% [8, 9]).

We studied petrography of two thin sections of MIL 05035, 31 and LAP 02224, 28 using a scanning electron microscope (Hitachi 3400 II) in the back-scattered electron imaging mode. Mineral compositions were measured with the JEOL 8100 electron microprobe at Nanjing University. The operating conditions are 15 kV accelerating voltage and 20 nA beam current. Peak and background counting times are 10 and 5 s for most elements, respectively. Natural and synthetic standards were used, and all data were reduced by the ZAF procedure. Cathodoluminescence (CL) images were made by using a CL device attached to the microprobe mentioned above.

Raman spectra of minerals were acquired at Nanjing University with a Renishaw RM2000 micro-Raman spectrometer equipped with a CCD detector. The operating conditions were: excitation laser wavelength: 514 nm (Ar^+ laser), laser energy: 5 mW, and spectral slit: 25 μm. The 50× objective was used on a Leica DM/LM microscope. With this objective, the lateral spot-size of the laser beam was about 1 μm. Silicon (520 cm^{-1} Raman shift) was used as a standard.

Uranogenic Pb/Pb dating of zirconolite and baddeleyite was performed using a CAMECA IMS-1280 secondary ion mass spectrometer (SIMS) at the Institute of Geology and Geophysics of the Chinese Academy of Sciences. The multicollector mode was used to determine Pb/Pb ages of zirconolite and baddeleyite without external standardization. Note however, that U-Pb system concordance cannot be checked by this method because U isotopes were not determined. The O_2^- primary ion beam was accelerated at –13 kV, with an intensity of ca. 100 pA. To obtain this small beam size, a Gaussian illumination mode was used. The ellipsoidal spot is about 5 μm in size. Positive secondary ions were extracted with a 10 kV potential. Oxygen flooding was used to increase the O_2 pressure to ~5×10^{-6} Torr in the sample chamber to enhance Pb^+ sensitivity. The multicollector mode with four electron multipliers was used to measure secondary ion beam intensities of ^{204}Pb, ^{206}Pb, ^{207}Pb, and $^{90}Zr_2{}^{16}O_2$ with integration times of 6 s. Each measurement consists of 60 cycles. A NMR controller was used to stabilize the magnetic field. The mass resolution power is fixed to 8000 (defined at 50% peak height). Relative yield of each electron multiplier was calibrated with Pb isotopes of a Phalaborwa baddeleyite standard [10]. Before measuring secondary ions, an area of 20 μm× 20 μm was sputtered by a 2 nA primary ion beam to remove possible contaminants. Detailed procedures were described in ref. [5]. Standard deviation of $^{207}Pb/^{206}Pb$ in the Phalaborwa baddeleyite standard is 0.52%. The assigned analytical error is based on the greater of the standard deviation of the Phalaborwa standard and analytical error of counting statistics of unknown samples. Correction of common Pb was made by measuring ^{204}Pb. Due to common Pb having multiple sources (e.g., initial Pb, sample preparation), it is difficult to estimate precise common Pb composition, so we assume common lead composition as $^{206}Pb/^{204}Pb = 14\pm4$ and $^{207}Pb/^{206}Pb = 0.84\pm 0.2$. Only data with $^{206}Pb/^{204}Pb > 1000$ are accepted for calculation of ages.

3 Results

3.1 Petrography and mineralogy of MIL 05035

MIL 05035 has a typical gabbro texture and consists mainly of coarse-grained pyroxene and plagioclase. Pyroxene grains in MIL 05035 show chemical heterogeneity or contain exsolution lamellae. Fine-grained fayalite-hedenbergite-silica symplectites are common and usually occur along margins of pyroxene. Silica, apatite, and K-Si-rich glass also exist in the section. No magnesian olivine was observed. However, fayalitic olivine occurs with high-Ca augite partially enclosed in coarse-grained low-Ca augite. Coarse-grained minerals (especially pyroxene) are severely fractured. Radial fractures occur along the rim of plagioclase enclosed in pyroxene. All plagioclase grains have been transformed into maskelynite. Opaque minerals are spinel, ilmenite, troilite, and minor zirconolite and baddeleyite. Zirconolite and baddeleyite occur as euhedral grains in a groundmass of silica and K-Si-rich glass (Figure 1(a)).

Pyroxenes have a chemical variation from pigeonite to high-Ca augite and to hedenbergite (Table 1; Figure 2(a)). All pyroxenes are Fe-rich with $Mg^{\#}$ (molecular Mg/(Mg+Fe) ratio) values varying from 0.53 (core) to 0.08 (rim). Hedenbergite in symplectites has an $Mg^{\#}$ range of 0.1–0.16 and high Wo values (39.4–42.7). High-Ca augite coexisting with fayalitic olivine contains higher Wo component ($Wo_{42.7}En_{23.6}Fs_{33.7}$) than those enclosing them ($Wo_{25.3–29.3}En_{24.5–24.8}Fs_{46–49.9}$). Plagioclase is anorthitic and has a limited compositional variation ($An_{90.1–92.7}Ab_{7.2–9.6}$). Fayalite in symplectites and coexisting with ilmenite and ulvöspinel has an $Mg^{\#}$ value of 0.05 to 0.07, whereas faya-

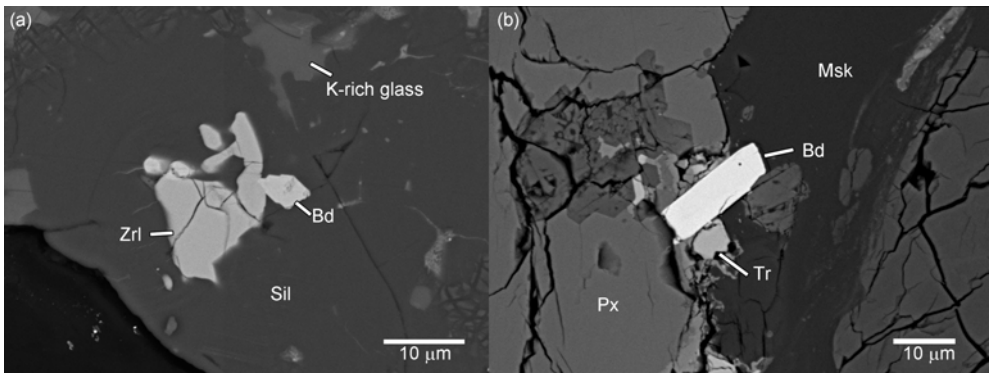

Figure 1 Back-scattered electron (BSE) images of Zr-minerals. (a) Zirconolite and baddeleyite are enclosed by groundmass of silica and K-rich glass. (b) A baddeleyite lath occurs in the interstice between pyroxene and maskelynite. Px, pyroxene; Msk, maskelynite; Sil, silica; Tr, troilite; Zrl, zirconolite; Bd, baddeleyite.

Table 1 Representative compositions of minerals and glass in MIL 05035 (wt%)[a)]

	cpx						ilm	pl	ol	ol	usp	sil	gl
SiO_2	49.0	48.1	49.3	46.8	46.4	46.3	bd	45.0	30.0	31.3	0.03	96.7	49.2
TiO_2	0.86	0.99	0.71	0.85	0.94	0.85	52.4	0.02	0.29	0.05	28.1	0.24	1.23
Al_2O_3	1.80	1.57	1.16	0.99	0.83	0.93	0.02	35.4	0.02	0.03	3.30	0.82	23.5
Cr_2O_3	0.63	0.39	0.38	0.05	0.04	0.08	0.30	bd	bd	0.03	8.09	0.03	0.02
MgO	13.2	9.75	12.0	5.18	1.48	3.13	0.15	0.05	1.85	7.76	0.57	bd	0.30
FeO	23.0	22.1	28.3	33.6	32.6	35.4	46.7	0.67	66.8	58.7	58.7	1.07	7.95
MnO	0.50	0.46	0.51	0.59	0.42	0.54	0.49	bd	0.99	0.71	0.51	bd	0.06
CaO	10.3	15.1	7.14	10.9	16.8	12.4	bd	18.5	0.35	0.59	bd	0.14	14.7
K_2O	bd	bd	bd	bd	bd	bd	bd	0.10	bd	bd	bd	0.30	0.29
Na_2O	0.02	bd	0.02	0.03	0.04	0.03	bd	0.99	bd	0.02	bd	0.05	0.93
Total	99.3	98.5	99.5	99.0	99.6	99.7	100.1	100.7	100.3	99.2	99.3	99.4	98.2
$Mg^{\#}$	0.51	0.44	0.43	0.22	0.08	0.14			0.05	0.19			
Wo	22.1	32.8	15.6		38.0	28.0				Chr	12.2		
En	39.5	29.7	36.5		4.7	9.9				Spl	7.4		
Fs	38.3	37.5	47.9		57.3	62.1				Usp	80.4		
An								92.5					

a) cpx, clinopyroxene; ilm, ilmenite; pl, plagioclase; ol, olivine; usp, ulvöspinel; sil, silica; gl, glass; bd, below detection limit; Wo=1000×Ca/(Ca+Mg+Fe) mol ratio; En=100×Mg/(Ca+Mg+Fe) mole ratio; Fs=100×Fe/(Ca+Mg+Fe) mole ratio; An=100×Ca/(Ca+Na+K) mole ratio; Chr=100×Cr/(Cr+Al+2Ti) mole ratio; Spl=100×Al/(Cr+Al+2Ti) mole ratio; Usp=100×2Ti/(Cr+Al+2Ti) mole ratio. The same below.

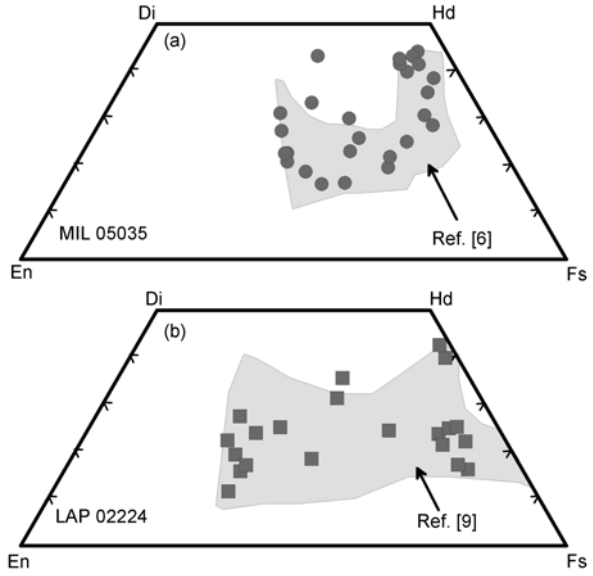

Figure 2 Chemical compositions of pyroxenes in MIL 05035 and LAP 02224 lunar meteorites.

litic olivine coexisting with high-Ca augite is relatively Mg-rich ($Mg^{\#}$=0.19). Ilmenite is compositionally close to pure $FeTiO_3$ with low MgO content (0.13 wt%–0.77 wt%). Spinel is dominated by an ulvöspinel component ($Usp_{77.4–80.4}Chr_{12.2–15.1}Spl_{7.4–8.1}$). The mineralogy is of agreement with previous investigations [6, 7], suggesting that MIL 05035 is of lunar origin.

3.2 Petrography and mineralogy of LAP 02224

LAP 02224 shows a typical subophitic basaltic texture, consisting dominantly of pyroxene, plagioclase, and ilmenite. Magnesian olivine grains are subhedral to euhedral in shape and usually contain melt or mineral inclusions. Both pyroxene and olivine exhibit chemical zoning. No exsolution lamellae occur in pyroxenes. Plagioclase has partially transformed to maskelynite or shows undulatory extinction. Spinel occurs as inclusions in olivine or as interstitial grains. A few spinel grains show chemical zoning. Mesostasis is common and contains fayalite and K-Si-rich glass with a

'Swiss-cheese' texture. Minor silica, troilite (with FeNi metal), phosphate minerals, and baddeleyite also occur as late-stage phases (Figure 1(b)). Most minerals (e.g., pyroxene, plagioclase, ilmenite, and olivine) have irregular fractures that could be caused by shock.

Corresponding to their chemical zoning, pyroxenes have a wide compositional range ($Wo_{11.1–42.2}En_{1.6–55.8}Fs_{27.2–74.7}$, $Mg^{\#}$=0.03–0.65; Table 2, Figure 2(b)). Within a few grains, pyroxene varies from low-Ca augite (core) to high-Ca augite through pyroxferroite, and then to hedenbergite (rim). Pyroxene in one inclusion of olivine contains higher Al_2O_3 (9.34 wt%) and TiO_2 (2.14 wt%) than other pyroxenes. Olivine also has a large chemical variation from core (Fo_{67}) to rim (Fo_{23}). Fayalite (Fo_1) in the mesostasis has a composition close to end member. Plagioclase in LAP 02224 is sodic anorthite ($An_{84.5–88.3}Ab_{10.9–12.9}$). Spinel has a large compositional variation within individual grains or between different grains ($Usp_{13.3–87.8}Chr_{6.8–60.9}Spl_{5.6–25.8}$). However, most spinel grains are dominated by an ulvöspinel component. Ilmenite has near end-member compositions with very low MgO (0.04 wt%–0.23 wt%). The mineralogy is of agreement with previous investigations [8, 9], suggesting that LAP 02224 is of lunar origin.

Raman spectra (8 spots) of two baddeleyite grains were acquired (Figure 3). The spectra show strong and sharp peaks at 1090, 1145, 1220, and 1270 cm^{-1}. A few peaks with less intensity occur in 200–600 cm^{-1} and their Raman shifts are the same. These features indicate that the two baddeleyite grains were not vitrified.

3.3 SIMS Pb/Pb age of zirconolite and baddeleyite

Four SIMS spots were analyzed on one zirconolite grain in MIL 05035 and nine spots on two baddeleyite grains in LAP 02224. The results are given in Table 3. Four analyses of zirconolite in MIL 05035 gave almost identical results within analytical errors and yield a weighted mean $^{207}Pb/^{206}Pb$ age of 3851±8 Ma (2σ) (Figure 4). The two baddeleyite grains in LAP 02224 have different Pb/Pb ages.

Table 2 Representative compositions of minerals and glass in LAP 02224 (wt%)[a)]

	ol			cpx				
SiO_2	36.4	31.6	29.6	45.0	50.6	51.3	49.9	47.6
TiO_2	0.04	0.11	0.20	2.14	0.88	0.41	0.94	1.56
Al_2O_3	bd	bd	0.04	9.34	2.34	0.97	2.12	2.04
Cr_2O_3	0.03	bd	0.04	0.03	0.80	0.44	0.64	0.20
MgO	30.96	9.41	0.38	12.1	17.0	19.2	15.0	7.40
FeO	31.6	57.3	67.5	19.6	18.4	20.5	19.3	24.5
MnO	0.39	0.72	0.93	0.42	0.44	0.47	0.35	0.42
CaO	bd	0.04	0.94	10.6	8.89	5.37	11.1	16.0
K_2O	bd	bd	bd	bd	bd	bd	bd	bd
Na_2O	bd	0.04	bd	0.08	bd	bd	0.05	0.07
Total	99.4	99.2	99.6	99.3	99.4	98.7	99.4	99.8
$Mg^{\#}$	0.64	0.23	0.01	0.53	0.62	0.63	0.58	0.35
Wo				24.8	19.0	11.1	23.5	35.2
En				39.5	50.6	55.8	44.6	22.8
Fs				35.7	30.4	33.0	31.9	42.0

	cpx		gl	pl	Kfs	ox		
SiO_2	46.4	46.7	61.4	47.8	76.3	0.07	0.07	bd
TiO_2	0.64	1.04	0.52	0.05	0.46	5.28	30.7	52.7
Al_2O_3	0.61	0.91	22.5	31.9	13.0	12.7	2.64	0.08
Cr_2O_3	0.04	bd	0.03	bd	bd	44.8	4.89	0.06
MgO	2.90	0.58	0.56	0.28	bd	1.66	0.10	0.04
FeO	40.8	33.2	3.00	0.71	2.03	35.6	60.3	46.2
MnO	0.67	0.49	0.05	bd	bd	0.37	0.47	0.43
CaO	6.72	17.4	5.56	17.9	1.84	0.04	bd	bd
K_2O	bd	bd	2.42	0.06	7.18	bd	bd	bd
Na_2O	0.04	0.03	1.28	1.33	0.24	bd	bd	0.02
Total	98.8	100.4	97.3	100.0	101.0	100.5	99.2	99.5
$Mg^{\#}$	0.11	0.03						
Wo	15.8	39.5			Chr	60.8	7.3	
En	9.5	1.8			Spl	25.6	5.9	
Fs	74.7	58.7			Usp	13.6	86.9	
An				87.9				

a) ol, olivine; cpx, clinopyroxene; gl, glass; pl, plagioclase; Kfs, K-feldspar; ox, oxide; bd, below detection limit.

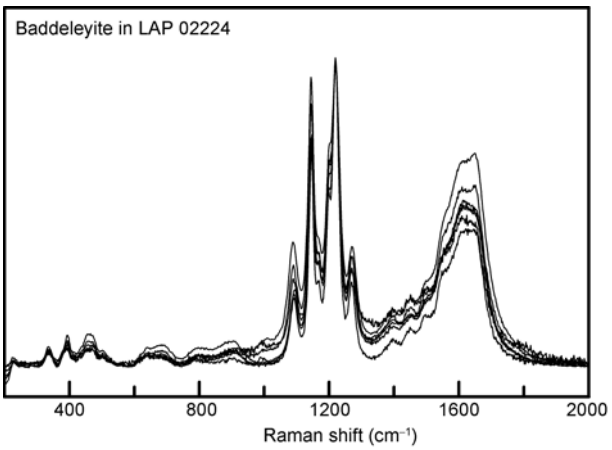

Figure 3 Raman spectra (200–2000 cm^{-1}) of baddeleyite in LAP 02224.

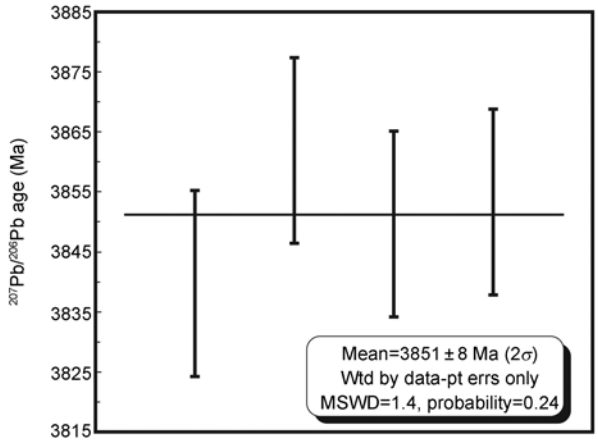

Figure 4 Weighted mean $^{207}Pb/^{206}Pb$ age of zirconolite in MIL 05035.

The big baddeleyite grain (Figure 5(a), 6 μm×20 μm) shows a large internal variation of Pb/Pb age, from 3109±29 Ma (2σ) to 3547±21 Ma (2σ). The oldest and youngest ages correspond to the brightest and darkest areas of the CL image (Figure 5(b)), whereas the other ages correspond to analytical spots on both bright and dark areas. Four results on the other baddeleyite grain are identical within analytical errors (Figure 6(a)), and the weighted mean $^{207}Pb/^{206}Pb$ age is 3005±17 Ma (2σ) (Figure 6(b)).

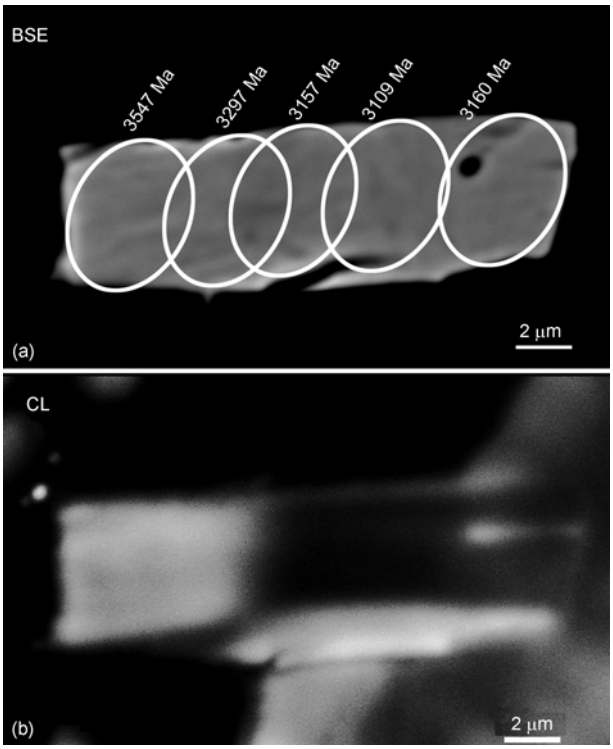

Figure 5 Back-scattered electron (BSE) (a) and CL (b) images of a baddeleyite grain in LAP 02224. The ellipsoidal circles indicate the SIMS spot locations. Bright areas in the CL image are older than darker areas.

Table 3 SIMS Pb/Pb data of zirconolite in MIL 05035 and of baddeleyite in LAP 02224[a)]

Sample spot	$^{206}Pb^{\#}/^{204}Pb_m$	±1σ(%)	$^{207}Pb^{\#}/^{206}Pb_m$	±1σ(%)	$^{207}Pb^{\&}/^{206}Pb_c$	±1σ(%)	$t_{207/206}$ (Ma)	±2σ
MIL 05035 zirconolite								
MIL@1	3439	14	0.3801	0.38	0.3820	0.52	3840	15
MIL@2	6536	14	0.3848	0.38	0.3877	0.52	3862	15
MIL@3	9346	12	0.3814	0.17	0.3845	0.52	3850	15
MIL@4	18939	12	0.3820	0.17	0.3855	0.52	3853	15
LAP 02224 baddeleyite grain-1								
LAP@1	5742	22	0.2451	0.66	0.2437	0.67	3160	21
LAP@2	4770	26	0.2377	0.89	0.2359	0.92	3109	29
LAP@3	2381	13	0.2692	0.58	0.2686	0.61	3297	19
LAP@4	1515	17	0.3169	0.65	0.3152	0.69	3547	21
LAP@5	4706	17	0.2451	0.57	0.2433	0.59	3157	19
LAP 02224 baddeleyite grain-2								
LAP2@1	1986	10	0.2275	0.56	0.2232	0.61	3020	19
LAP2@2	2673	11	0.2252	0.52	0.2220	0.55	3011	18
LAP2@3	3234	17	0.2239	0.81	0.2212	0.84	3005	27
LAP2@4	3912	15	0.2206	0.55	0.2184	0.58	2985	18

a) $^{206}Pb_m{}^{\#}/^{204}Pb$ and $^{207}Pb^{\#}/^{206}Pb_m$ are the measured values. $^{207}Pb^{\&}/^{206}Pb_c$ is the calculated value after common-lead correction, assuming that common Pb composition as $^{206}Pb/^{204}Pb$ = 14±4, $^{207}Pb/^{206}Pb$ = 0.84±0.2.

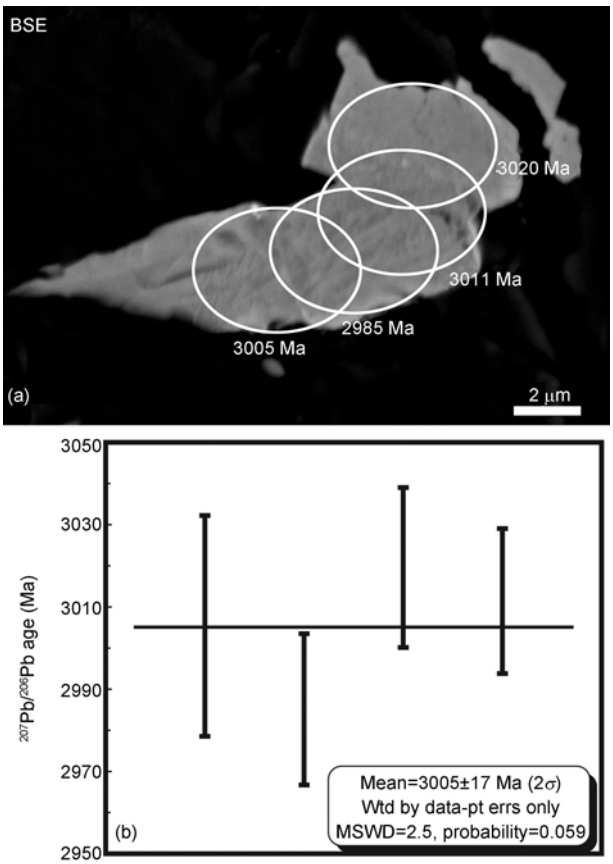

Figure 6 Back-scattered electron image (a) and weighted mean $^{207}Pb/^{206}Pb$ age (b) of a baddeleyite grain in LAP 02224. The ellipsoidal circles indicate the SIMS spot locations.

4 Discussion

4.1 Crystallization ages of MIL 05035 and LAP 02224

Our zirconolite Pb/Pb age of 3.851±0.008 Ga in MIL 05035 is indistinguishable, with a much improved precision, from previously reported whole the rock-mineral Sm-Nd age of 3.80±0.05 Ga and the Rb-Sr isochron age of 3.90±0.04 Ga [11]. Plagioclase in MIL 05035 has transformed into maskelynite, indicating heavily shock metamorphism; however, lack of recrystallization in maskelynite implies a very short duration of high pressure and high temperature. Although the closure temperature of zirconolite remains unknown [12], the U-Pb system in zirconolite probably was not affected by impact due to slow diffusion rate of Pb in Zr-rich minerals [13]. The consistency of ages from different methods indicates that these ages may represent the crystallization age of parent magma of MIL 05035.

The two baddeleyite grains in LAP 02224 show a large variation in Pb/Pb age. In one grain, the variation is from 3.109 to 3.547 Ga and corresponds to the change of brightness in the CL image. This feature indicates that the U-Pb system in baddeleyite could have been disturbed by late thermal events after its crystallization. Nyquist et al. [14] determined the age of LAP 02205, a paired stone of LAP 02224 with Rb-Sr, Ar/Ar, and Sm-Nd methods. The Rb-Sr and Ar/Ar data give an age of ~3.02±0.03 Ga (2σ) and 2.955±0.010 Ga (1σ) for LAP 02205, respectively; whereas the Sm-Nd data suggests an older age of 3.15±0.02 Ga [14]. In situ U-Pb analysis of phosphate in LAP 02205 gave an even younger age of 2.93±0.15 Ga [15]. Compared to these ages, the oldest baddeleyite Pb/Pb age (3.55 Ga) of LAP 02224 could be the minimum of crystallization age of parent magma of the LAP lunar meteorites; whereas the younger ages (~3.1 and ~3 Ga) could reflect the time of thermal event(s) and are not the crystallization age.

4.2 Pairing possibility with other lunar meteorites

Among the crystalline lunar basalt meteorites, Asuka 881757 and Yamato 793169 have a crystallization age similar to that of MIL 05035. Misawa et al. [16] reported ages of 3.798±0.012 Ga (Ar/Ar) to 3.940 ± 0.028 Ga (Pb/Pb) for Asuka 881757 by a series of analytical methods. Torigoye-Kita et al. [17] reported a U-Th-Pb age of 3.8 Ga for Yamato 793169, which probably represents its crystallization. The younger Sm-Nd (3.4 Ga) and Ar/Ar ages for Yamato 793169 could be caused by subsequent metamorphic events. Taken the face value, the identical crystallization ages suggest that MIL 05035, Asuka 881757, and Yamato 793169 may originate from the same locality on the Moon. Furthermore, the similarity in petrography, mineralogy, and Sm-Nd and Rb-Sr isotopic systematics also suggests that MIL 05035 could be launch-paired with Asuka 881757 [11, 16, 18]. Difference in initial ε_{Nd} values implies that MIL 05035 (+7.2±0.4 [11]) and Asuka 881757 (+7.4± 0.5 [15]) could originate from different depth from that of Yamato 793169 (+3.9±0.3 [16]). This conclusion is consistent with the observation of pyroxene texture and zoning trend [18]. Furthermore, solar-wind derived noble gas and exposure age indicated that Asuka 881757 and Yamato 793169 might have been ejected in different events [19].

LAP 02224 has similar petrographic features to Dhofar 287A, and the crystallization age ($\geqslant$3.55 Ga) of LAP 02224 is close to crystallization ages of lunar basalt meteorite Dhofar 287A (phosphate U-Pb age of 3.34±0.2 Ga and Pb/Pb age of 3.35±0.13 Ga [20]) within analytical errors. However, phosphate U-Pb ages of the two lunar meteorites (LAP 02205 [15] and Dhofar 287A [20]) are different and LAP 02224 contains higher REE concentrations than Dhofar 287A [8, 9]. These differences argue against them being paired. Jolliff et al. [21] suggested that LAP 02205 (the pairing stone of LAP 02224) resembled NWA 032 (a low-Ti mare basalt meteorite) and could be launch-paired with it. However, the petrography of LAP 02224 is different from that of NWA 032 (Figure 4 in ref. [22]), which has a finer-grained groundmass. Borg et al. [23] measured the Rb-Sr (2.852±0.065 Ga) and Sm-Nd (2.692±0.16 Ga)

isochron ages of NWA 032, which are much younger than the Rb-Sr and Sm-Nd ages of LAP 02205 [14] and the baddeleyite Pb/Pb age of LAP 02224 in this study. Thus, although the Ar/Ar age of NWA 032 is similar to that of LAP 02205, it is not likely that NWA 032 is paired with the LAP lunar meteorites. Therefore, the LAP lunar meteorites are probably unique and not paired with other known lunar meteorites.

4.3 Possible source regions and origins

Among the samples collected by Apollo and LUNA missions, only the Apollo 11 and 17 samples contain old mare basalts up to 3.7–3.9 Ga, comparable to MIL 05035 and Asuka 881757 [11]. However, most of these Apollo mare basalts are high-Ti basalts (TiO_2>6 wt%) [24]. Although very low-Ti basalts were also discovered amongst the Apollo 17 samples, olivine in these basalts is Mg-rich ($Fo_{76–53}$ [24]), in sharp contrast to those in MIL 05035 and Asuka 881757. Thus, MIL 05035 could not have been derived from the same source of the Apollo and LUNA mare basalts. Hiesinger et al. [25, 26] reported crater size-frequency ages of lunar nearside mare basalts. Among the studied nearside mare basalts, the probable source regions for MIL 05035 are the southwest of mare Australe (A1 ~3.88 Ga or A2 ~3.80 Ga), the middle part (HU1 ~3.84/3.94 Ga, HU2 and HU3 ~3.77 Ga) in mare Humboldtianum based only on age similarity. However, combining Ti concentration and $(^{87}Rb/^{86}Sr)_{source}$ ratio, the most probable source for MIL 05035 is the mare Australe [11].

Based on isochron ages and geochemical data, Nyquist et al. [14] suggested LAP 02205 could have formed in a source region near the Apollo 12 site. However, the baddeleyite Pb/Pb age ($\geqslant$3.55 Ga) of LAP 02224 is much older than Apollo 12 low-Ti basalts (~3.15 Ga [27]). Since the precise crystallization age of LAP 02224 remains unknown, the possible source region of LAP lunar meteorites will still be an open question.

Great efforts have been made to establish the correlation between chemical compositions (bulk TiO_2) of mare basalts and crystallization ages [28]. Except a few pre-mare basalts having ages of 3.9 to 4.35 Ga (aluminous low-Ti basalt [1]; very low-Ti basalt [2]), Apollo 11 and 17 high-Ti mare basalts are relatively old, ranging in age from 3.5–3.9 Ga. Low-Ti (1.5 wt%–6 wt% TiO_2) mare basalt samples are younger in the range of 3.1 to 3.4 Ga. And most very low-Ti basalts (<1.5 wt% TiO_2) are much younger (e.g., 3.2–3.3 Ga for LUNA 24). Our LAP 02224 crystallization age is much older than most other low-Ti mare basalts, indicating that low-Ti basaltic volcanism seems to have spanned a longer duration than has been thought [29, 30]. MIL 05035 is also older than most very low-Ti mare basalts (e.g., LUNA 24), indicating that very low-Ti basalts have a large variation in age (2.9–3.9 Ga) [11, 16, 17, 31] and a long duration (~1 Ga) of volcanism.

Previous investigations show that MIL 05035 is depleted in incompatible elements including the rare earth elements [6, 9]. Thus, the magmatic event related to MIL 05035 source region might not be due to decay of radiogenic elements, although MIL 05035 is old. Heating by shock impact could be more likely since the crystallization age (~3.9 Ga) of MIL 05035 is consistent with the peak age of impact bombardment of the Moon. As LAP 02224 has relatively high incompatible element concentrations [9]; its origin is probably related to radiogenic heating in the Procellarum KREEP Terrane.

The authors thank NASA Meteorites Working Group for providing the two thin sections studied here. We are also grateful to Prof. Xianhua Li for his constructive comments. The manuscript also benefit from comments from two reviewers. This study was supported by State Key Laboratory of Lithospheric Evolution at the Institute of Geology and Geophysics, Chinese Academy of Sciences, National Natural Science Foundation of China (Grants Nos. 40703015, 40773046), and Minor Planet Foundation of China.

1 Taylor L A, Shervais J W, Hunter R H, et al. Pre-4.2 AE mare-basalt volcanism in the lunar highlands. Earth Planet Sci Lett, 1983, 66: 33–47
2 Terada K, Anand M, Sokol A K, et al. Cryptomare magmatism at 4.35 Ga recorded in Kalahari 009. Nature, 2007, 450: 849–852
3 Korotev R L. Lunar geochemistry as told by lunar meteorites. Chemie der Erde, 2005, 65: 297–346
4 Rasmussen B, Fletcher I R, Muhling J R. Pb/Pb geochronology, petrography and chemistry of Zr-rich accessory minerals (zirconolite, tranquillityite and baddeleyite) in mare basalt 10047. Geochim Cosmochim Acta, 2008, 72: 5799–5818
5 Li X H, Liu Y, Li Q L, et al. Precise determination of Phanerozoic zircon Pb/Pb age by multicollector SIMS without external standardization. Geochem Geophys Geosys, 2009, 10: Q04010, doi: 10.1029/2009GC002400
6 Joy K H, Crawford I A, Anand M, et al. The petrology and geochemistry of Miller Range 05035: A new lunar gabbroic meteorite. Geochimt Cosmochim Acta, 2008, 72: 3822–3844
7 Liu Y, Floss C, Day J M D, et al. Petrogenesis of lunar mare basalt meteorite Miller Range 05035. Meteor Planet Sci, 2009, 44: 262–284
8 Day J M D, Taylor L A, Floss C, et al. Comparative petrology, geochemistry, and petrogenesis of evolved, low-Ti lunar mare basalt meteorites from the LaPaz Icefield, Antarctica. Geochim Cosmochim Acta, 2006, 70: 1581–1600
9 Joy K H, Crawford I A, Downes H, et al. A petrological, mineralogical, and chemical analysis of the lunar mare basalt meteorite LaPaz Icefield 02205, 02224, and 02226. Meteor Planet Sci, 2006, 41: 1003–1025
10 Heaman L M. The application of U-Pb geochronology to mafic, ultramafic and alkaline rocks: An evaluation of three mineral standards. Chem Geol, 2009, 261: 43–52
11 Nyquist L E, Shih C Y, Reese Y D. Sm-Nd and Rb-Sr ages for MIL 05035: Implications for surface and mantle sources. Lunar Planet Sci, 2007, XXXVIII: Abstract #1702
12 Rajesh V J, Yokoyama K, Santosh M, et al. Zirconolite and baddeleyite in an ultramafic suite from southern India: Early Ordovician carbonatite-type melts associated with extensional collapse of the Gondwana crust. J Geol, 2006, 114: 171–188
13 Lee J K W, Williams I S, Ellis D J. Pb, U and Th diffusion in natural zircon. Nature, 1997, 390: 159–162
14 Nyquist L E, Shih C Y, Reese Y D, et al. Age of lunar meteorite LAP 02205 and implications for impact-sampling of planetary surfaces. Lunar Planet Sci, 2005, XXXVI: Abstract #1374

15 Anand M, Taylor L A, Floss C, et al. Petrology and geochemistry of LaPaz Icefield 02205: A new unique low-Ti mare-basalt meteorite. Geochim Cosmochim Acta, 2006, 70: 246–264
16 Misawa K, Tatsumoto M, Dalrymple G B, et al. An extremely low U/Pb source in the Moon: U-Th-Pb, Sm-Nd, Rb-Sr, and $^{40}Ar/^{39}Ar$ isotopic systematics and age of lunar meteorite Asuka 881757. Geochim Cosmochim Acta, 1993, 57: 4687–4702
17 Torigoye-Kita N, Misawa K, Dalrymple G B, et al. Further evidence for a low U/Pb source in the Moon: U-Th-Pb, Sm-Nd, and Ar-Ar isotopic systematics of lunar meteorite Yamato 793169. Geochim Cosmochim Acta, 1995, 59: 2621–2632
18 Koeberl C, Kurat G, Brandstätter F. Gabbroic lunar mare meteorites Asuka-881757 (Asuka-31) and Yamato 793169: Geochemical and mineralogical study. Proc NIPR Symp Antarct Meteor, 1993, 6: 14–34
19 Takeda H, Arai T, Saiki K. Mineralogical studies of lunar meteorite Yamato-793169, a mare basalt. Proc NIPR Symp Antarct Meteor, 1993, 6: 3–13
20 Terada K, Sasaki Y, Anand M, et al. Uranium-lead systematic of low-Ti basaltic meteorite Dhofar 287A: Affinity to Apollo 15 green glasses. Earth Planet Sci Lett, 2008, 270: 119−124
21 Jolliff B L, Zeigler R A, Korotev R L. Petrography of lunar meteorite LAP 02205, a new low-Ti basalt possibly launch paired with NWA 032. Lunar Planet Sci, 2004, XXXV: Abstract #1438
22 Fagan T J, Taylor G J, Keil K, et al. Northwest Africa 032: Product of lunar volcanism. Meteor Planet Sci, 2002, 37: 371–394
23 Borg L, Gaffney A, DePaolo D. Rb-Sr & Sm-Nd isotopic systematic of NWA 032. 70th Annual Meteoritical Society Meeting, 2007. Abstract #5232
24 Papike J J, Ryder G, Shearer C K. Lunar samples. Rev Mineral, 1998, 36: 5.1–5.234
25 Hiesinger H, Jaumann R, Neukum G, et al. Ages of mare basalts on the lunar nearside. J Geophys Res, 2000, 105(E12): 29239–29275
26 Hiesinger H, Head J W, Wolf U, et al. Ages and straigraphy of mare basalts in Oceanus Procellarum, Mare Nubium, Mare Cognitum, and Mare Insularum. J Geophys Res, 2003, 108(E7): 5065, doi: 10.1029/2002JE001985
27 Stöffler D, Ryder G, Ivanov B A, et al. Cratering history and lunar chronology. Rev Mineral Geochem, 2006, 60: 519–596
28 Snyder G A, Borg L E, Nyquist L E, et al. Chronology and isotopic constraints on lunar evolution. In: Canup R, Righter K, eds. Origin of the Earth and Moon. Tucson: University of Arizona Press, 2000. 361–395
29 Day J M D, Floss C, Taylor L A, et al. Evolved mare basalt magmatism, high Mg/Fe feldspathic crust, chondritic impactors, and the petrogenesis of Antarctic lunar breccia meteorites Meteorite Hills 01210 and Pecora Escarpment 02007. Geochim Cosmochim Acta, 2006, 70: 5957–5989
30 Terada K, Sasaki T, Anand M, et al. Uranium-lead systematic of phosphates in lunar basaltic regolith breccia, Meteorite Hills 01210. Earth Planet Sci Lett, 2007, 259: 77−84
31 Nyquist L E, Shih C Y, Reese Y D, et al. Sm-Nd and Rb-Sr ages and isotopic systematic for NWA 2977, a young basalt from the PKT. Meteor Planet Sci, 2009, 44: A157